Front. Phys. 13(4), 137305 (2018)
https://doi.org/10.1007/s11467-018-0786-y

RESEARCH ARTICLE

Temperature dependence of the excitonic spectra of monolayer transition metal dichalcogenides

Zi-Wu Wang†, Run-Ze Li, Xi-Ying Dong, Yao Xiao, Zhi-Qing Li

Tianjin Key Laboratory of Low Dimensional Materials Physics and Preparing Technology, Department of Physics, Tianjin University, Tianjin 300354, China
Corresponding author. E-mail: †wangziwu@tju.edu.cn
Received December 21, 2017; accepted March 28, 2018

We theoretically study the temperature dependence of the excitonic spectra of monolayer transition metal dichalcogenides using the O′Donnell equation, $E_g(T) = E_g(0) - S\langle\hbar\omega\rangle[\coth(\frac{\langle\hbar\omega\rangle}{2k_BT} - 1)]$. We develop a theoretical model for the quantitative estimation of the Huang–Rhys factor S and average phonon energy $\langle\hbar\omega\rangle$ based on exciton coupling with longitudinal optical and acoustic phonons in the Fröhlich and deformation potential mechanisms, respectively. We present reasonable explanations for the fitted values of the Huang–Rhys factor and average phonon energy adopted in experiments. Comparison with experimental results reveals that the temperature dependence of the peak position in the excitonic spectra can be well reproduced by modulating the polarization parameter and deformation potential constant.

Keywords transition metal dichalcogenides, exciton, Huang–Rhys factor

PACS numbers 73.20.Mf, 78.20.Bh, 79.60.Jv

1 Introduction

Reduced dimensionality and decreased dielectric screening result in the remarkable exciton effect in monolayer transition metal dichalcogenides (TMDs), which has recently attracted increasing attention [1, 2]. Excitons are elementary quasiparticles representing the electronic response to optical excitation; they play a dominant role in determining the optical properties of these materials. Many optical properties, such as the coherence time, population decay, and many-body effects, are reflected in the excitonic spectra. Therefore, an understanding of the excitonic spectra is crucial for using these monolayer materials in potential electronic and optoelectronic applications.

There have been several experimental measurements of the excitonic spectra [3–9]. In particular, the temperature dependence of the spectra has been studied widely by different experimental methods, revealing that the peak positions of the spectra are red-shifted with increasing temperature. To explain this phenomenon, the O′Donnell equation, $E_g(T) = E_g(0) - S\langle\hbar\omega\rangle[\coth(\frac{\langle\hbar\omega\rangle}{2k_BT} - 1)]$, is extensively employed [10], where $E_g(0)$ denotes the zero temperature exciton energy, $\langle\hbar\omega\rangle$ represents the average phonon energy (APE) contributing to the temperature change of the exciton energy, and S is the Huang–Rhys factor (HRF), which describes the effective strength of electron-phonon coupling. The best-fitting values of these parameters are deduced for different monolayer TMDs materials. The temperature dependence of the excitonic spectra is well fitted in experiments. However, the detailed processes for calculating these fitting parameters and the conditions that yield these best-fitting values in theory have not been presented.

Using the Huang–Rhys model, we develop theoretical processes for estimating the HRF and APE based on exciton coupling with both longitudinal acoustic (LA) and longitudinal optical (LO) phonons in monolayer TMDs materials via the deformation potential and Fröhlich mechanisms, respectively. We discuss the dependence of the HRF and APE on the cutoff wave number (COWN) of the phonon modes, the deformation potential constant, and the polarization parameter. The best-fitting values for the HRF and APE adopted in experiments can be obtained by modulating the deformation potential constant and polarization parameter. We present theoretical simulations of the temperature dependence of the excitonic spectra of monolayer MoS_2 and $MoSe_2$. The

dominant features of the experimentally observed temperature dependence are well reproduced. The developed theoretical model not only provides a reasonable explanation for the excitonic spectra, but also may be widely applied to study the spectral properties of monolayer structures.

2 Theoretical model

We assume that the optical transitions start from the exciton ground state in the emission spectrum of monolayer TMDs, where the exciton states are generally described by the standard two-dimensional Wannier–Mott model. The charge density of the exciton ground state, which consists of a localized hole and an electron, can be expressed as [11–13]

$$\rho(r) = \rho_h(r) - \rho_e(r), \tag{1}$$

with

$$\rho_h(r) = \delta(r),$$
$$\rho_e(r) = \frac{4}{a_0} \cdot \exp\left(-\frac{2a_0}{r}\right),$$

where r is the coordinate of the relative electron-hole motion, and $a_0 = \varepsilon_r a_B/\mu$ is the effective exciton Bohr radius, which is related to the relative static dielectric constant (ε_r) and reduced exciton mass (μ). The Hamiltonian of exciton coupling with phonons can be given as

$$H_{ex-ph} = \sum_{\lambda=LO,LA} \sum_k M_\lambda(k)(a_k + a_{-k}^\dagger)\mathrm{e}^{\mathrm{i}k\cdot r}, \tag{2}$$

with the coupling element

$$M_{LO}(k) = \sqrt{\frac{(e^2\eta_0 L_m \hbar\omega_{LO})}{(2A\varepsilon_0)}} erfc\left(\frac{k\sigma}{2}\right),$$

for the LO phonon mode in the Fröhlich mechanism [14, 15] and as

$$M_{LA}(k) = \mathrm{i}\sqrt{\frac{D^2\hbar k}{2A\varrho\omega_{LA}}} erfc\left(\frac{k\sigma}{2}\right)$$

for the LA phonon mode in the deformation potential mechanism [14, 15]. Here a_k ($a_k^\dagger$) is annihilation (creation) a phonon with wave number k; e is the carrier charge; η_0 is the polarization parameter, which is determined by the polarization properties of monolayer TMDs; L_m is the monolayer thickness; A is the quantization area in the monolayer plane; and ε_0 is the permittivity of vacuum. $erfc$ is the complementary error function, σ is the effective width of the electronic Bloch states on the basis of the constrained interaction of the phonon with charge carriers in monolayer materials, D is the deformation potential constant for the LA phonon, and ϱ is the mass density. ω_{LO} and ω_{LA} are the frequency of the LO and LA phonons, respectively. In this paper, we assume that the LO phonon mode has a single frequency and the LA phonon follows the linear dispersion $\omega_{LA} = c_{LA}k$ (c_{LA} is the sound velocity). These parameters used in the theoretical calculation are listed in Table 1 [16–18].

Following the Huang–Rhys model [19], the amplitude of the HRF due to exciton-phonon coupling can be expressed as

$$V_\lambda(k) = M_\lambda(k) \int \mathrm{e}^{\mathrm{i}k\cdot r}\rho(r)\mathrm{d}r, \tag{3}$$

which makes it possible to calculate the HRF as

$$S_\lambda = \sum_{\lambda=LO,LA} \sum_k \frac{1}{(\hbar\omega_\lambda)^2}|V_\lambda(k)|^2. \tag{4}$$

In polar coordinates, $V_\lambda(k)$ is expressed as

$$V_\lambda(k) = M_\lambda(k) \int J_0(kr)\rho(r)\mathrm{d}r. \tag{5}$$

By performing the integral in Eq. (5) and converting the summation of the wave number (k) into the integral in Eq. (4), the HRFs of the LO and LA phonon modes can be given as

$$S_{LO} = \int_0^{k_c} \frac{e^2\eta_0 L_m}{4\pi\varepsilon_0\hbar\omega_{LO}} \left| erfc\left(\frac{k\sigma}{2}\right)\right|^2 \widetilde{F}(a_0,k)k\mathrm{d}k, \tag{6}$$

$$S_{LA} = \int_0^{k_c} \frac{D^2}{4\pi\hbar\varrho c_{LA}^3} \left| erfc\left(\frac{k\sigma}{2}\right)\right|^2 \widetilde{F}(a_0,k)\mathrm{d}k, \tag{7}$$

Table 1 Parameters adopted for the theoretical calculation of the HRF and average phonon energy in monolayer MoS_2 and $MoSe_2$. The effective width of the electronic Bloch states, $\sigma = 0.44$ nm, and the monolayer thickness, $L_m = 0.6$ nm, are those adopted for monolayer MoS_2 and $MoSe_2$ in the calculation process. In addition, the spectra of the A-type exciton is selected as an example in this paper. Parameters were taken from Refs. [16, 17], and [18].

Quantity	$E_g(0)$	$\hbar\omega_{LO}$ (phonon energy)	μ (reduce mass)	ε_r (dielectric constant)	ϱ (mass density)	c_{LA} (sound velocity)
MoS_2	1.95 (eV)	48 (meV)	$0.27(m_0)$	$4.26(\varepsilon_0)$	1.56×10^{-7} (g/cm^2)	6.7×10^3 (m/s)
$MoSe_2$	1.67 (eV)	34 (meV)	$0.34(m_0)$	$4.74(\varepsilon_0)$	2.01×10^{-7} (g/cm^2)	4.1×10^3 (m/s)

with

$$\widetilde{F}(a_0,k)=\frac{5+4k^2/a_0^2-4\sqrt{1+4k^2/a_0^2}}{1+4k^2/a_0^2},$$

where k_c is the COWN of the phonon mode.

3 Results and discussion

Figure 1 shows the dependence of the HRFs of the LO (S_{LO}) and LA (S_{LA}) phonon modes in monolayer MoS_2 on the COWN. The HRFs increase with increasing COWN. However, they increase very little after the COWN reaches 6×10^9 m^{-1} and 2×10^9 m^{-1} for the LO and LA phonon modes, respectively, indicating that the long-wavelength phonon modes make the predominant contributions to the HRF. (In the following calculation, we choose 6×10^9 m^{-1} as the effective COWN for the two phonon modes.) From Fig. 1(a), one can also see that S_{LO} obviously increases with increasing polarization parameter (η_0). The polarization parameter generally describes the coupling strength between charge carriers and LO phonons, which is determined by the dielectric constants of the material in the Fröhlich mechanism and has been chosen as a fixed value in previous studies [14, 15, 17, 18]. We define it as a variable because it is related to many parameters in monolayer materials, such as the dielectric environment, dimensional confinement, and screening effects, increasing the challenge of estimating its value accurately. Recently, Sohier *et al.* theoretically studied a similar coupling strength in monolayer TMDs using a density functional perturbation calculation and concluded that the two-dimensional Fröhlich coupling is much stronger than was assumed in previous *ab initio* studies [20]. Moreover, the new parameter g_{Fr} was defined as the coupling strength and

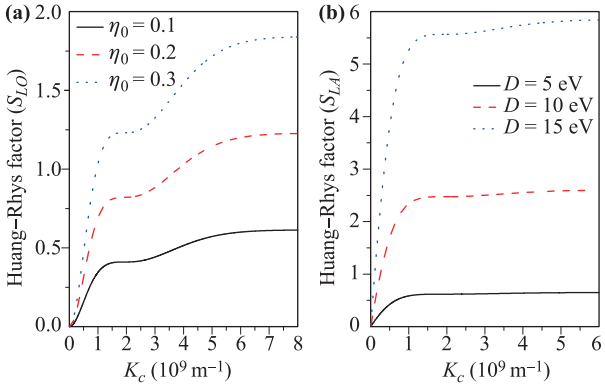

Fig. 1 **(a)** HRF of LO phonon mode (S_{LO}) as a function of the COWN (k_c) at different polarization parameters; **(b)** HRF of LA phonon mode (S_{LA}) as a function of the COWN at different deformation potential parameters.

can also be varied on a very large scale. Nevertheless, quantitative comparisons of η_0 and g_{Fr} are not given in this paper and need to be explored further. The effect of the deformation potential constant on S_{LA} is plotted in Fig. 1(b); the deformation potential constant (D) strongly affects the value of S_{LA}, which reflects the fact that the coupling strength between charge carriers and LA phonons modes is greatly modified by this constant. Several fixed values have been adopted in previous studies [14, 15]. In fact, determining its value accurately is also a difficult task in experiments.

To fit the temperature dependence of the peak positions in the excitonic spectra via the O′Donnell equation, the effective HRF (S) and APE ($\langle\hbar\omega\rangle$) have been adopted in experiments, for example, $S=1.82$, 2.29, 2.2 and $S=1.93$, 1.96, 2.24, as well as $\langle\hbar\omega\rangle=22.5$, 24.25, 23 meV and $\langle\hbar\omega\rangle=11.6$, 15 meV for monolayer MoS_2 and $MoSe_2$, respectively [3–9]. However, how and under what conditions these fitting parameters were obtained were not given. We determine the average contributions of the LO and LA phonon modes in the Huang–Rhys model and redefine these two fitting parameters as

$$S_{average}=\frac{S_{LO}\hbar\omega_{LO}+S_{LA}\langle\hbar\omega_{LA}^{ar}\rangle}{\hbar\omega_{LO}+\langle\hbar\omega_{LA}^{ar}\rangle}, \tag{8}$$

$$\langle\hbar\omega\rangle=\frac{S_{LO}\hbar\omega_{LO}+S_{LA}\langle\hbar\omega_{LA}^{ar}\rangle}{S_{LO}+S_{LA}}, \tag{9}$$

where $\langle\hbar\omega_{LA}^{ar}\rangle$ is the average energy of the LA phonon mode and is obtained via

$$\langle\hbar\omega_{LA}^{ar}\rangle=\frac{\sum_k S_{LA}\hbar\omega_{LA}}{\sum_k S_{LA}}. \tag{10}$$

The dependence of $\langle\hbar\omega_{LA}^{ar}\rangle$ on the COWN (k_c) is shown in Fig. 2(a). The value of $\langle\hbar\omega_{LA}^{ar}\rangle$ reaches 3.8 meV and then changes little as $k_c>6\times10^9$ m^{-1}. Moreover, the value of $\langle\hbar\omega_{LA}^{ar}\rangle$ is independent of the deformation potential constant inferred from Eq. (10). In Ref. [3], average phonon energies of tens of milli-electron volts were adopted to fit the experimental results. Such large values for $\langle\hbar\omega_{LA}^{ar}\rangle$ are rarely obtained if only the contribution of the LA phonon mode is considered, even if the transverse acoustic phonon modes are included. Therefore, the contributions of optical phonon modes need to be taken into account. The numerical results for the HRF and APE obtained by averaging the contributions of the LO and LA phonon modes in Eqs. (8) and (9) are plotted in Figs. 2(b) and (c), respectively. These best-fitting values of the HRF and APE in experiments can be obtained by choosing appropriate values of the polarization parameter and deformation potential constant. Hence, the summations of the exciton coupling with LO and LA phonons can give reasonable values of the fitting parameters in the O′Donnell equation in experiments expected. In addition, these theoretical results also pro-

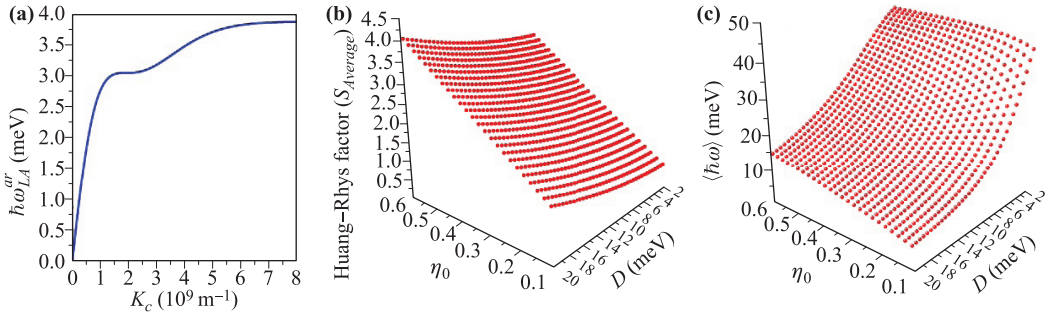

Fig. 2 **(a)** Average energy of LA phonon mode as a function of the COWN; **(b)** HRF as functions of the polarization parameter and deformation potential constant; **(c)** average phonon energy as functions of the polarization parameter and deformation potential constant.

vide a quantitative comparison with first-principle calculations of the HRF and APE.

Substituting these fitting parameters obtained from Eqs. (8) and (9) into the O′Donnell equation, we present theoretical simulations of the temperature dependence of the peak position in monolayer MoS_2 in Figs. 3(a) and (b). Experimental excitonic spectra often exhibit two remarkable features. One is that the shift in the peak position is not pronounced when the temperature is 0–100 K. From Figs. 3(a) and (b), we can see that this feature is well reproduced and can be modulated appropriately by the deformation potential constant and polarization parameter. Another feature is that the peak position varies by several tens of milli-electron volts in experiments, which can also be well fitted by controlling the deformation potential constant and polarization parameter. Figures 3(c) and (d) show the theoretical temperature dependence of the peak positions in monolayer $MoSe_2$, in which the two features are also well reproduced. Therefore, both these fitting parameters and the temperature dependence of the excitonic spectra of monolayer TMDs are more reasonably explained by the proposed model. This model could be suitable for studying the excitonic spectra of other two-dimensional materials. In this paper, we take into account mainly the LO and LA phonon modes, which couple much more strongly with excitons than other phonon modes do. In fact, the coupling between excitons in monolayer TMDs and the surface optical phonon modes induced by polar substrates are strongly enhanced [21, 22]. The influence of these phonon modes on the temperature dependence of the excitonic spectra should be considered in future work.

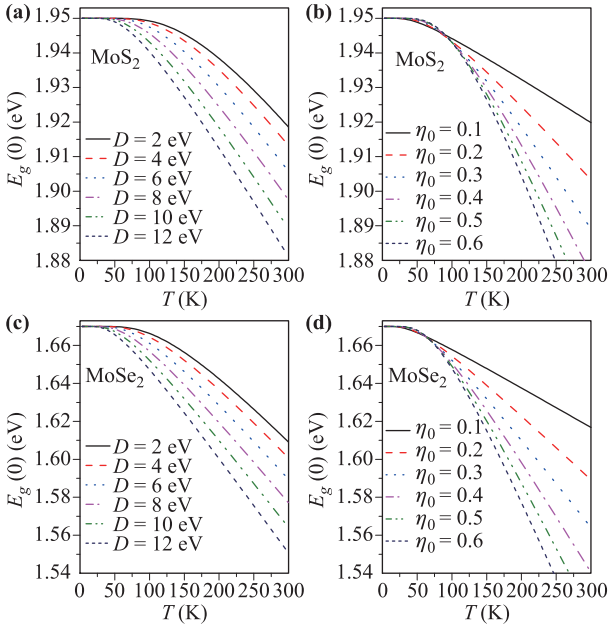

Fig. 3 Peak position as a function of temperature for **(a)**, **(c)** different deformation potential constants at $\eta_0 = 0.3$ and **(b)**, **(d)** different polarization parameters at $D = 10$ eV in (a), (b) monolayer MoS_2 and (c), (d) monolayer $MoSe_2$.

4 Conclusion

In conclusion, we develop the Huang–Rhys model to calculate the effective HRF and APE in the O′Donnell equation based on coupling between excitons and LO and LA phonons. We find that these long-wavelength phonons make the dominant contribution to the HRF and APE. The values of the HRF and APE adopted in experiments on monolayer TMDs are obtained reasonably well by averaging the contributions of the LO and LA phonon modes. Two remarkable features of the temperature dependence of the peak position are well reproduced by modulating the polarization parameter and deformation potential constant. The theoretical results provide understanding of the exciton state and its optical properties in these monolayer materials.

Acknowledgements This work was supported by the National Natural Science Foundation of China (Grant No. 11674241) and Young Core Instructor of Peiyang (Grant No. 11303267).

References

1. H. Y. Yu, X. D. Cui, X. D. Xu, and W. Yao, Valley excitons in two-dimensional semiconductors, *Natl. Sci. Rev.* 2(1), 57 (2015)
2. A. V. Kolobov and J. Tominaga, Two-dimensional transition-metal dichalcogenides, *Springer Series in Materials Science* 239, 321 (2016)
3. S. Tongay, J. Zhou, C. Ataca, K. Lo, T. S. Matthews, J. Li, J. C. Grossman, and J. Wu, Thermally driven crossover from indirect toward direct bandgap in 2D semiconductors: $MoSe_2$ versus MoS_2, *Nano Lett.* 12(11), 5576 (2012)
4. J. S. Ross, S. F. Wu, H. Y. Yu, N J. Ghimire, A. M. Jones, G. Aivazian, J. Q. Yan, D. G. Mandrus, D. Xiao, W. Yao, and X. D. Xu, Electrical control of neutral and charged excitons in a monolayer semiconductor, *Nature Commun.* **4**, 1474 (2013)
5. A. P. S. Gaur, S. Sahoo, J. F. Scott, and R. S. Katiyar, Electron–phonon interaction and double-resonance raman studies in monolayer WS_2, *J. Phys. Chem. C* 119(9), 5146 (2015)
6. A. Arora, M. Koperski, K. Nogajewski, J. Marcus, C. Faugeras, and M. Potemski, Excitonic resonances in thin films of WSe_2: From monolayer to bulk material, *Nanoscale* 7(23), 10421 (2015)
7. A. A. Mitioglu, K. Galkowski, A. Surrente, L. Klopotowski, D. Dumcenco, A. Kis, D. K. Maude, and P. Plochocka, Magnetoexcitons in large area CVD-grown monolayer MoS_2 and $MoSe_2$ on sapphire, *Phys. Rev. B* 93(16), 165412 (2016)
8. P. Dey, J. Paul, Z. Wang, C. E. Stevens, C. Liu, A. H. Romero, J. Shan, D. J. Hilton, and D. Karaiskaj, Optical coherence in atomic-monolayer transition-metal dichalcogenides limited by electron-phonon interactions, *Phys. Rev. Lett.* 116(12), 127402 (2016)
9. J. W. Christopher, B. B. Goldberg, and A. K. Swan, Long tailed trions in monolayer MoS_2: Temperature dependent asymmetry and resulting red-shift of trion photoluminescence spectra, *Sci. Rep.* 7(1), 14062 (2017)
10. K. P. O'Donnell and X. Chen, Temperature dependence of semiconductor band gaps, *Appl. Phys. Lett.* 58(25), 2924 (1991)
11. K. L. He, N. Kumar, L. Zhao, Z. F. Wang, K. F. Mak, H. Zhao, and J. Shan, Tightly bound excitons in monolayer WSe_2, *Phys. Rev. Lett.* 113(2), 026803 (2014)
12. A. Chernikov, T. C. Berkelbach, H. M. Hill, A. Rigosi, Y. L. Li, O. B. Aslan, D. R. Reichman, M. S. Hybertsen, and T. F. Heinz, Exciton binding energy and nonhydrogenic Rydberg series in monolayer WS_2, *Phys. Rev. Lett.* 113(7), 076802 (2014)
13. T. Olsen, S. Latini, F. Rasmussen, and K. S. Thygesen, Simple screened hydrogen model of excitons in two-dimensional materials, *Phys. Rev. Lett.* 116(5), 056401 (2016)
14. K. Kaasbjerg, K. S. Thygesen, and K. W. Jacobsen, Phonon-limited mobility in n-type single-layer MoS_2 from first principles, *Phys. Rev. B* 85(11), 115317 (2012)
15. K. Kaasbjerg, K. S. Bhargavi, and S. S. Kubakaddi, Hot-electron cooling by acoustic and optical phonons in monolayers of MoS_2 and other transition-metal dichalcogenides, *Phys. Rev. B* 90(16), 165436 (2014)
16. A. Ramasubramaniam, Large excitonic effects in monolayers of molybdenum and tungsten dichalcogenides, *Phys. Rev. B* 86(11), 115409 (2012)
17. A. Thilagam, Ultrafast exciton relaxation in monolayer transition metal dichalcogenides, *J. Appl. Phys.* 119(16), 164306 (2016)
18. A. Thilagam, Exciton formation assisted by longitudinal optical phonons in monolayer transition metal dichalcogenides, *J. Appl. Phys.* 120(12), 124306 (2016)
19. M. C. Klein, F. Hache, D. Ricard, and C. Flytzanis, Size dependence of electron-phonon coupling in semiconductor nanospheres: The case of CdSe, *Phys. Rev. B* 42(17), 11123 (1990)
20. T. Sohier, M. Calandra, and F. Mauri, Two-dimensional Fröhlich interaction in transition-metal dichalcogenide monolayers: Theoretical modeling and first-principles calculations, *Phys. Rev. B* 94(8), 085415 (2016)
21. C. Jin, J. Kim, J. Suh, Z. Shi, B. Chen, X. Fan, M. Kam, K. Watanabe, T. Taniguchi, S. Tongay, A. Zettl, J. Q. Wu, and F. Wang, Interlayer electron-phonon coupling in WSe_2/hBN heterostructures, *Nat. Phys.* 13, 127 (2017)
22. C. M. Chow, H. Y. Yu, A. M. Jones, J. Q. Yan, D. G. Mandrus, T. Taniguchi, K. Watanabe, W. Yao, and X. D. Xu, Unusual exciton–phonon interactions at van der Waals engineered interfaces, *Nano Lett.* 17(2), 1194 (2017)